Separation Science and Technology
Publication details, including instructions for authors and subscription information:
http://www.informaworld.com/smpp/title~content=t713708471

Removal of As(V) and Cr(VI) Ions from Aqueous Solution using a Continuous, Hybrid Field-Gradient Magnetic Separation Device

Ashish K. Jha[a]; Arijit Bose[a]; Jerome P. Downey[b]
[a] Department of Chemical Engineering, University of Rhode Island, Kingston, RI, USA [b] Hazen Research, Golden, CO, USA

To cite this Article Jha, Ashish K. , Bose, Arijit and Downey, Jerome P.(2006) 'Removal of As(V) and Cr(VI) Ions from Aqueous Solution using a Continuous, Hybrid Field-Gradient Magnetic Separation Device', Separation Science and Technology, 41: 15, 3297 — 3312
To link to this Article: DOI: 10.1080/01496390600915007
URL: http://dx.doi.org/10.1080/01496390600915007

Separation Science and Technology, 41: 3297–3312, 2006

ISSN 0149-6395 print/1520-5754 online
DOI: 10.1080/01496390600915007

Removal of As(V) and Cr(VI) Ions from Aqueous Solution using a Continuous, Hybrid Field-Gradient Magnetic Separation Device

Ashish K. Jha and Arijit Bose
Department of Chemical Engineering, University of Rhode Island, Kingston, RI, USA

Jerome P. Downey
Hazen Research, Golden, CO, USA

Abstract: A continuous flow colloidal affinity magnetic separation device is used for the removal of As(V) and Cr(VI) from aqueous solutions. Langmuir isotherms fit the adsorption behavior of the individual ions on Orica MIEX® ion exchange particles. In a mixture of equal weight percent As(V) and Cr(VI), the adsorption of As(V) begins only above a critical cut-off concentration, implying preferential adsorption of the higher valence ion at the available sites. Cr(VI) is removed selectively from the mixture in the continuous flow device, consistent with the presence of a higher concentration of the higher valence ion in the proximity of a charged (anion-exchange) surface.

Keywords: Magnetic separation, ion-exchange

INTRODUCTION

Magnetic separation methods rely on labeling target material with magnetic particles and mobilizing these particles to specific locations using magnetic field gradients. This process is versatile and can be used for a wide variety

Received 30 January 2006, Accepted 22 June 2006
Address correspondence to Arijit Bose, Department of Chemical Engineering, University of Rhode Island, Kingston, RI 02881, USA. Tel.: 401-874-2804; E-mail: bosea@egr.uri.edu

of separations because of the diversity in the choice of the affinity ligands that can be mounted on the surface of the magnetic particles. This principle has been widely used in the area of immunomagnetic separation, where antibodies are immobilized on magnetic carriers for capturing target cells (1).

These separations are typically conducted in batch mode. The force on a magnetic particle exerted by an external field is proportional to the gradient of the field. Typical decay lengths associated with magnetic fields created using common permanent or electromagnets are of the order of $\sim$1 cm (2). This puts a restriction on the dimensions of the container used for batch processing. The volumetric limitation can be overcome by employing devices that operate in the continuous, rather than the batch mode. To this end, a magnetic quadrupole field cell sorter was developed (3). This device is amenable to a continuous separation process because an outward radial force acts on the magnetically labeled cells under quadrupole field. Dipole and quadrupole based separation devices have been designed (4), which fractionate magnetically labeled cells into different streams on the basis of the degree to which the cells are immunomagnetically tagged.

Ghebremeskel and Bose (5, 6). developed a device with an axially rotating horizontal tubular chamber equipped with a series of axially located magnetic units. Each magnetic unit consists of an alternating-current solenoid followed by an electromagnet. The tube rotates about its horizontal axis, which prevents settling of non-neutrally buoyant magnetic particles under gravity. The transient axial magnetic field generated by solenoids induces oscillation in the magnetic particles, which in turn causes them to mix intimately with the solution. The electromagnets draw the magnetic particles to the tube wall thereby separating them from the rest of the solution (7). The on-off cycle of the electromagnets are manipulated to enable the recovery of the trapped magnetic particles without interrupting the feed streams. Electromagnets, when energized, pull the target laden magnetic particles to the tube wall thereby separating them from the rest of the solution. When de-energized, electromagnets release the magnetic particles which are collected and sent to the stripping and the metal extraction cycle.

Heavy metal ions such as arsenic, cadmium, chromium, copper, lead, mercury, nickel, silver, and zinc represent some of the most common and notorious inorganic contaminants present in industrial wastewater (8). Arsenic and chromium are well known for their deleterious effects. Arsenic exposure is associated with skin and various internal cancers, cardiovascular, and neurological effects (9). Chromium (VI) is reported to be carcinogenic in humans and is toxic to aquatic life (10). Chromium is found in wastewaters originating at metal etching and plating operations, wood preservative manufacture, leather tanning industries, paint and pigments, dyeing, and steel fabrication (11,12). Sources of arsenic are petroleum refineries, fossil fuel power plants, nonferrous smelting activities and ceramics, semiconductors, pesticides, and fertilizer production (13). Chromium and arsenic have been identified as co-contaminants in wastes arising from wood preservative

manufacture, paint and ink manufacture, and petroleum refining, as well as in some municipal wastewaters. These heavy metals pose severe environmental and health concerns.

Conventional ion exchange methods have been used for the removal of these metals but they have disadvantages. For instance the pressure drop is very high as the solution has to be pumped through a stationary packed bed of resin. This requires special pumps. An alternate technique is to precipitate the metal ions from the solution. The disadvantage is that it introduces some additional contaminants (14). (such as sulfides in sulfide precipitation) and the metal is converted to a state from which processing and recovery are difficult. Also, different pH levels of minimum solubility for different metals add to the difficulty of being able to remove multiple ions simultaneously.

Magnetic separation can tackle the issue of wastewater treatment in a much more elegant way. Previous work from our laboratory (7) has focused on the removal of single metal ions from its aqueous solution. In this work, the separation of As(V) and Cr(VI) from an aqueous mixture using the continuous flow magnetic separation device is discussed. As(V) and Cr(VI) exist as anionic complexes (Cr(VI) as $Cr_2O_7^{-2}$ and $HCrO_4^{-1}$and As(V) as $H_2AsO_4^{-1}$ at pH $\sim$6) in an aqueous solution (15). Magnetic anion-exchange particles have been used for this study.

EXPERIMENTAL METHODS

Device Design

The schematic of the separation device built in our lab is shown in Fig. 1. The device consists of a 1.0 cm internal diameter, 1.2 m long axially-rotating

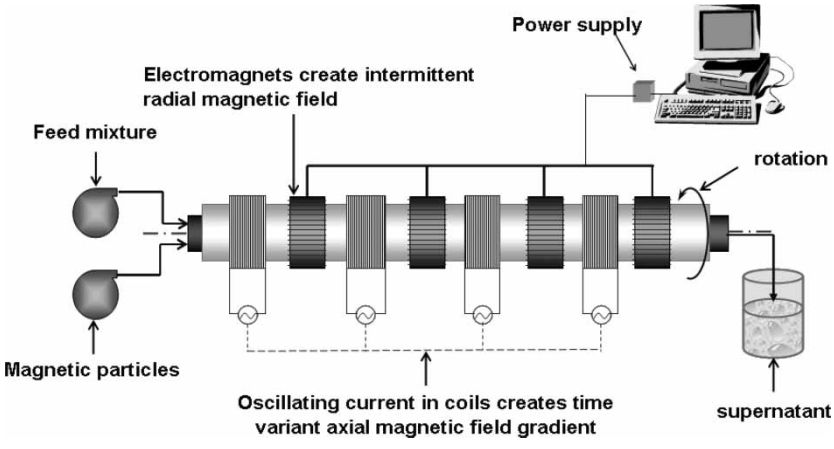

Figure 1. Schematic of magnetic separation device.

horizontal glass tube with four replicated magnetic units. Each unit consists of a stationary, alternating-current solenoid that surrounds the tube, followed by an electromagnet positioned at a distance of 4.0 cm from the solenoid. A ChronTrol-4S timer is used to control the on-off cycles of the electromagnets. A direct current (0.22 amps) flowing in the electromagnets generates radial magnetic field gradients within the tube, allowing magnetic particles to be drawn to the tube walls. Rotation of tube, at 25 rpm, retards the sedimentation of non-neutrally buoyant particles without introducing centrifugal forces. Two separate peristaltic pumps drive the feed mixture and the magnetic colloid suspension through a rotary coupler (Deublin, Inc.) into one end of the chamber. A second rotary coupler at the other end of the chamber allows the exiting liquid to flow into a stationary collection vessel.

Experiments

Magnetic ion exchange resin (MIEX®) was obtained from Orica Watercare as an aqueous slurry. The slurry was dried at 30°C and all calculations are based on the dry basis. Three solutions of varying arsenic and chromium concentrations were prepared to evaluate the effect of the presence of multiple ions on metal ions adsorption on the surface of the magnetic particles. The first contained 100 mg/l of Cr(VI), the second contained equal mass concentration of Cr(VI) and As(V) (100 mg/l each of As(V) and Cr(VI)), and the third contained 100 mg/l of As(V). Potassium dichromate ($K_2Cr_2O_7$) was used as a source for Cr(VI). Sodium hydrogen arsenate heptahydrate ($Na_2HAsO_4 \cdot 7H_2O$), (98%, A.C.S reagent from Sigma-Aldrich) was used as a source for As(V). All solutions were prepared using single distilled reverse osmosis water passed through a four cartridge Millipore "Milli Q" system until its resistivity reaches 18 MΩcm.

Batch experiments were conducted with each of the prepared solutions to obtain the equilibrium distribution (the adsorption isotherm) of ions between the aqueous phase and the surface of magnetic particles. In these experiments, a measured volume of the solution was exposed to an increasing amount of magnetic particles and stirred at room temperature (21°C) for about 30 minutes to equilibrate; the suspension was then left to settle for 2 hrs. Prior to metal analysis, the solution samples from each batch were filtered using 0.2 μm filter to remove any residual magnetic particles. Metal analysis was done using an Inductively Coupled Plasma Optical Emission Spectrometer (Perkin-Elmer Optima 3100 XL).

Metal removal experiments were conducted at an overall (sum of magnetic particles and feed flow rates) flow rate of 25 ml/min. In three different experiments, 200 ml aqueous solution of magnetic particles with an equal volume of sample was fed into the reactor using peristaltic pumps. The magnetic particle concentrations were 2 g/l, 2 g/l, and 4 g/l, and the metal ion concentrations were 30 mg/l of As(V), 30 mg/l of Cr(VI), and

30 mg/l both of As(V) and Cr(VI) respectively. The solutions were driven into the chamber through a rotary coupler. While the chamber rotated at 25 rpm, an alternating current (12 V, 10 A) passed through the solenoid, and the electromagnets were activated to draw the magnetic particles to the chamber wall. The supernatant flowing out through the end of the chamber was collected continuously for 10 min. In a timed sequence, the electromagnets were then turned off and remained inactive for 2 min. During this time, the target bound magnetic particles were driven out by the bulk flow and collected separately. The timer then restored current to the magnets to continue processing the solution.

Stage Optimization and Particle Regeneration

Stage optimization experiments were performed to maximize the removal of metal ion in a single stage at a particular flow rate. Four different experiments were done with 200 ml of 30 mg/l As(V) solution and an equal volume of magnetic particle solution at an overall flow rate of 25 ml/min. Magnetic particle loadings of 1 g/l, 2 g/l, 3 g/l, and 4 g/l were used.

In the regeneration experiments, the magnetic particles were first exposed to different metal ion solutions. The particles were separated from the solution using a magnet, and the samples were analyzed to determine the extent of particle saturation. The saturated particles were exposed to 1M NaCl solution in order to resolubilize the adsorbed ions and regenerate the ion exchange resin. The samples were analyzed to determine the extent of regeneration.

Characterization of the Magnetic Particles

The magnetic particles MIEX® from Orica Watercare were characterized to obtain their B-H characteristics. The particles were immobilized using wax in a small glass vial. They were then exposed to an increasing magnetic field and the corresponding particle magnetization was measured. The field was increased until saturation magnetization was reached. Then the direction of field was reversed to get the hysteresis behavior. The dipole moment of particles was evaluated using the saturation magnetization data. The magnetic potential energy between two particles was then evaluated as $2\,\mu B$ where μ is magnetization per unit volume multiplied by the volume of one particle, and B is field generated by the magnetic dipole at a distance of 2R from its centre where R is the radius of the magnetic particle. The size and morphology of the particles were obtained by scanning electron microscopy.

RESULTS AND DISCUSSIONS

Figures 2 and 3 show that the MIEX® resin absorption capacities for Cr(VI) and As(V) are 93 mg/g and 54 mg/g, respectively. Adsorption of lower amounts of As(V) as compared to Cr(VI) has also been reported on a different substrate (16). For experiments involving a mixture of the two metals, a decrease in saturation adsorption capacity for both metal ions was observed (Figs. 4 and 5), to 71 mg/g and 14 mg/g for Cr(VI) and As(V) respectively, consistent with the competitive adsorption of the two components in the solution (17). Figure 6 shows that the reduction in saturation adsorption capacity for As(V) is higher than that for Cr(VI). When a mixture of ions of different valency is exposed to a charged surface, the spatial distribution of ions favors a higher concentration of the higher valence ions at the surface (18). This is consistent with the observation here of greater relative adsorption of Cr(VI) than As(V) in the batch experiments.

The adsorption of As(V) and Cr(VI) has been found to follow the Langmuir isotherm on different substrates (19–21). For the MIEX particles used in these experiments, the adsorption data for the isotherms in Figs. 2, 3, 4, and 5 have been fitted to a Langmuir isotherm and shown in Figs. 7 and 8. Here, θ is the surface coverage (the ratio of the adsorbed metal concentration to the saturation metal concentration), C is the solution

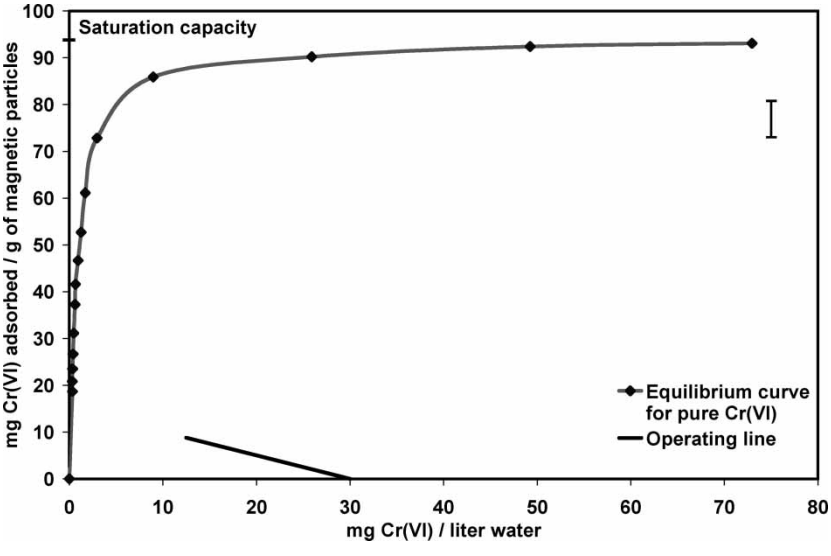

Figure 2. Pure Cr(VI) equilibrium curve and operating line. Equilibrium curve for pure Cr(VI) shows an adsorption capacity of 93 mg/g of particles. The operating line indicates inlet and outlet conditions. (The data points for all equilibrium isotherms have been connected through a smoothed line.)

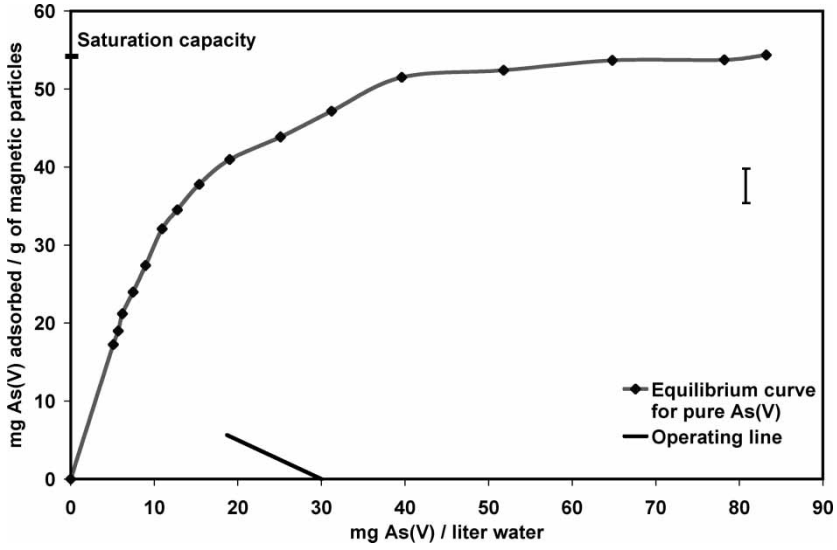

Figure 3. Pure As(V) equilibrium curve and operating line. Equilibrium curve for pure As(V) showing adsorption capacity of 54 mg/g of particles. The operating line indicates inlet and outlet conditions.

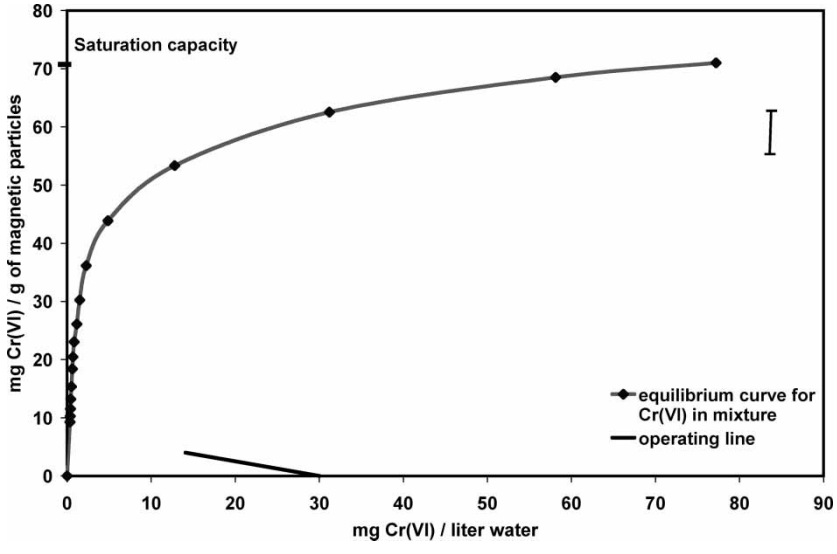

Figure 4. Equilibrium curve and operating line for Cr(VI) in a mixture. Equilibrium curve for Cr(VI) in equal mass concentration mixture of As(V) and Cr(VI) showing adsorption capacity of 71 mg/g of particles. The operating line indicates inlet and outlet conditions.

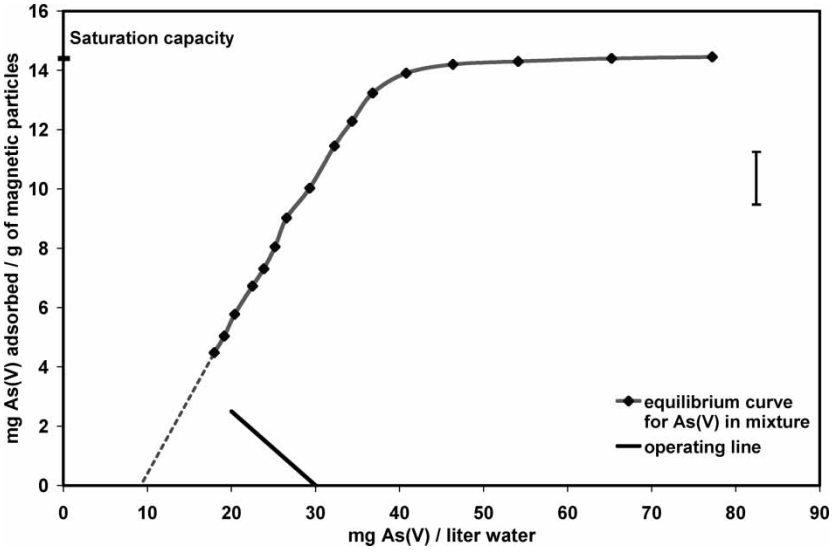

Figure 5. Equilibrium curve and operating line for As(V) in a mixture. Equilibrium curve for As(V) in equal mass concentration mixture of As(V) and Cr(VI) shows an adsorption capacity of ~14 mg/g of particles. Equilibrium curve extrapolation shows a cut-off concentration of ~9 mg/l, implying negligible As(V) adsorption below 9 mg/l concentration in the mixture. The operating line indicates inlet and outlet conditions.

metal concentration and b is the Langmuir parameter. For Cr(VI) the Langmuir parameter 'b' = 0.9985 $(mg/l)^{-1}$ and for As(V) 'b' = 0.1042 $(mg/l).^{-1}$ Since 'b' reflects the enthalpy of adsorption, Cr(VI) adsorbs much more strongly than As(V). The fit to Langmuir behavior is very poor

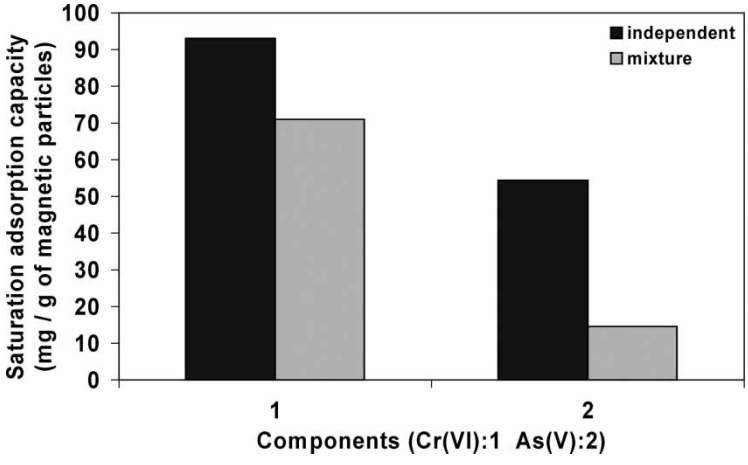

Figure 6. Comparison of adsorption capacities from single solutions and mixtures.

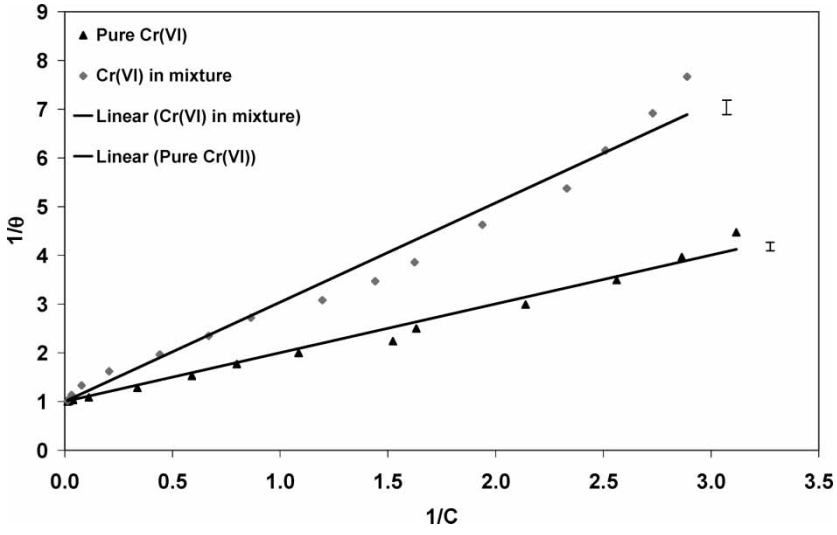

Figure 7. Langmuir fit for the adsorption of Cr(VI) on Orica MIEX particles.

for As(V) in mixture (Fig. 8), also apparent from the experimental isotherm (Fig. 5). The Langmuir isotherm description has been used just to compare the enthalpies of adsorption of As(V) and Cr(VI) on the magnetic particles substrate. In a mixture, the higher valence Cr(VI) competes for adsorption sites, and preferentially adsorbs until a critical concentration of As(V) of

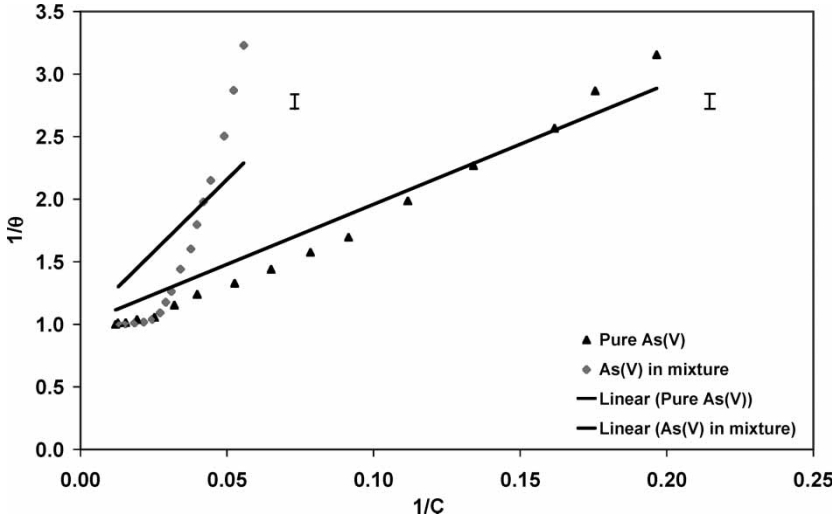

Figure 8. Langmuir fit for the adsorption of As(V) on Orica MIEX particles.

$\sim$9 mg/l. This is a case of a highly non-ideal adsorption system. We therefore exclude rigorous modeling of As(V) adsorption in a mixture from the scope of the present study.

Table 1 summarizes the metal removal results when solutions are flowed through the continuous device. Beginning with solutions that contained 30 mg/l of metal ions, one pass through the device removed 58.3% of Cr(VI), 37.6% of As(V), and 53% for Cr(VI) and 33.3% for As(V) in a 1:1 mixture (30 mg/l each). As the contaminant removal is a function of its concentration in the solution (8), even a single pass at low contaminant concentration might result in the desired removal efficiency.

Figures 2, 3, 4, and 5 show the operating lines for Cr(VI) removal, As(V) removal, and Cr(VI) and As(V) removal from mixture respectively. Operating lines have been obtained by monitoring concentrations at the inlet and exit of the device. The stage efficiency defined as percentage approach of the operating conditions to equilibrium was 51.8% and 57.1% for As(V) and Cr(VI) removal and 68.4% and 55.2% for As(V) and Cr(VI) removal from 1:1 (30 mg/l each) mixture.

A higher stage efficiency can be achieved by extending the residence time, either by reducing the solution flow rate, or by extending the chamber length. Reducing the flow rate hampers the process in terms of the output rate. Therefore, it is reasonable to operate the device at the maximum sustainable flow rate (maximum flow rate at which magnets do not lose particles) provided the reactor is made long enough to achieve the required residence time. Flow rate have been varied to find the optimum. In the current system, the maximum flow rate was approximately 35 ml/min before a significant magnetic particle breakthrough occurred. The experiments have been conducted at 25 ml/min to compensate for the length (1.2 m) of our lab prototype.

Figures 9 and 10 show the results of the stage optimization experiments. The target metal removal increased as a function of the magnetic particle concentration. With the 30 mg/l As(V) feed solution, the exiting concentration gradually decreased from 20.5 mg/l at 1 g/l magnetic particle loading to

Table 1. Summary of metal removal experiments

Component	Inlet stream conc. (mg/l)	Exit stream conc. (mg/l)	% Removal	% Stage efficiency
As(V)	30	18.7	37.6	51.8
Cr(VI)	30	12.5	58.3	57.1
As(V) in mixture	30	20	33.3	68.4
Cr(VI) in mixture	30	14.1	53	55.2

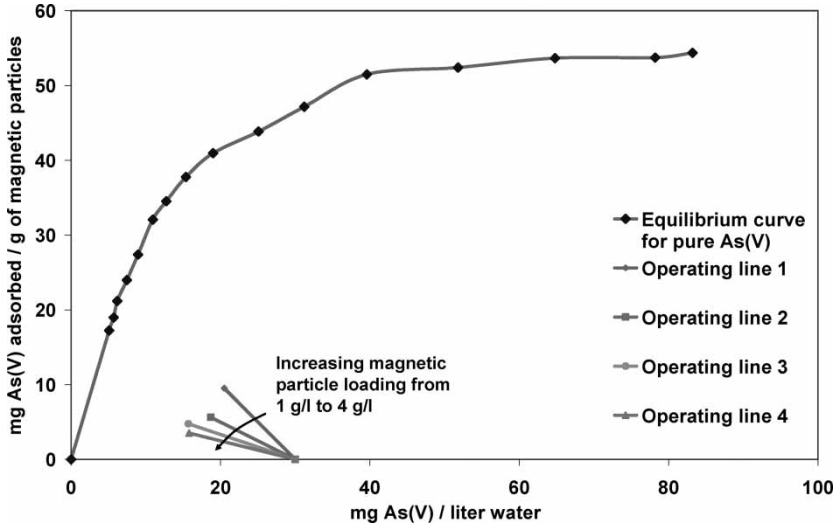

Figure 9. Stage optimization: Equilibrium curve for As(V) and operating lines corresponding to magnetic particle loading of 1g/l, 2g/l, 3g/l and 4g/l.

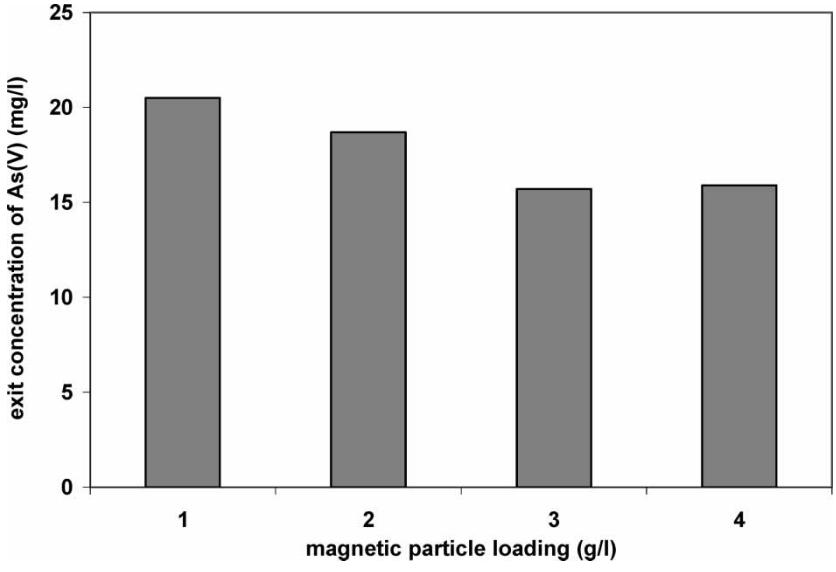

Figure 10. Change in exit concentration with particle loading. Exit concentration of a feed containing 30 mg/l As(V) solution vs. magnetic particle loading showing decreasing exit concentration with increasing loading with almost no change in exit concentration from 3g/l to 4g/l loading.

Table 2. Summary of particle regeneration experiments

Components	mg/g of magnetic particles before regeneration	mg/g of magnetic particles after regeneration	% Regeneration
Pure As(V)	50.16	2.70	94.6
As(V) in mixture	9.76	2.26	76.8
Pure Cr(VI)	95.08	23.50	75.3
Cr(VI) in mixture	58.53	14.35	75.5

15.7 mg/l at 3 g/l magnetic particle loading. Further increases in magnetic particle loading did not enhance As(V) removal. This suggests that the maximum removal of ions is limited by the adsorption kinetics. Also, clustering of magnetic particles at higher loadings will decrease the overall surface area available for adsorption. A scaled-up version of this device might get around some of these operational limitations. For example, increasing the reactor length will increase the residence time of magnetic particles, which in turn will increase the extent of adsorption of the target species.

Table 2 summarizes the results from regeneration experiment. Greater than 75% regeneration efficiency was achieved in all cases with the highest being 94.6% for pure As(V). These results suggest that the particles are suitable for regeneration and can be reused. Also, desorption of As(V) seems better than that of Cr(VI) (Fig. 11), which is in accordance with weaker adsorption of As(V) than

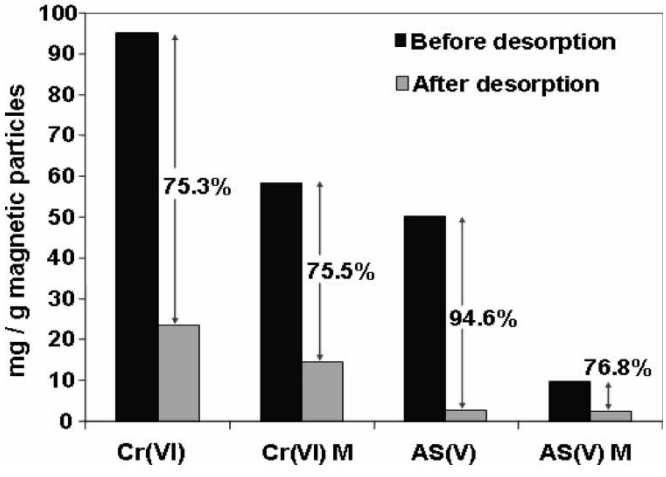

Figure 11. Desorption of ions from magnetic particles.

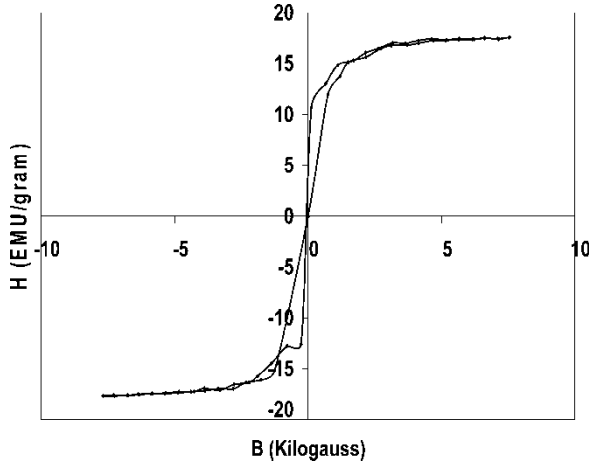

Figure 12. Magnetization-magnetic field (B-H) characteristic curve for MIEX® particles showing their paramagnetic behavior and a saturation magnetization of 17 EMU/g.

Cr(VI). Effective stripping and regeneration will be an economic necessity in metal extraction applications, such as wastewater treatment or when the target materials are precious metals such as gold, platinum and palladium.

The magnetic characterization of the particles is shown in Fig. 12. The saturation magnetization for MIEX® particles is17 EMU/g. No hysteresis

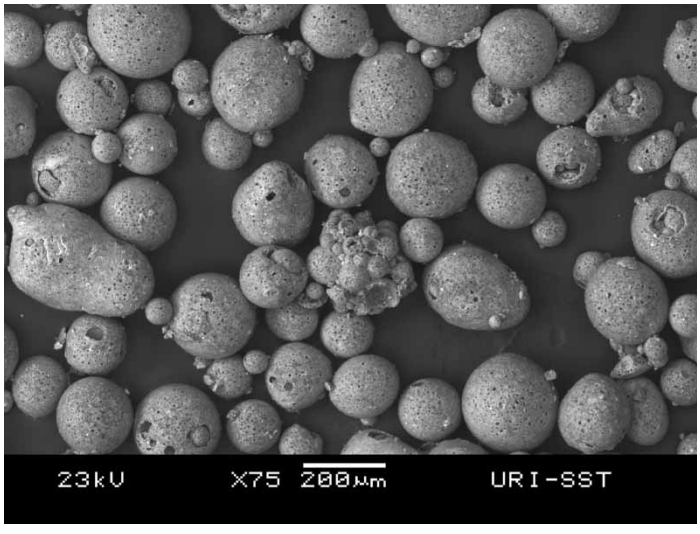

Figure 13. Scanning electron micrograph of MIEX® particles.

was observed, suggesting that the particles behave paramagnetically with negligible remnant magnetization in the absence of a magnetic field. An order of magnitude comparison was made between magnetic potential energy between two particles and the thermal energy kT that serves to randomize the magnetic dipole orientations. The calculations showed magnetic potential energy ($\sim 10^{-12}$ J) is nine orders of magnitude higher than kT ($\sim 10^{-21}$ J) suggesting that particles do actually tend to cluster under saturation conditions. Scanning Electron Microscopy showed that the particles are mostly spherical in shape with an average particle diameter of ~ 180 μm (Fig. 13). The BET surface area of these particles is ~ 15 m^2/g indicating that the particles are highly porous. The porosity allows the internal surface area to be available for adsorption, but also slows down the adsorption kinetics.

CONCLUSIONS

The experimental results demonstrated that the As(V) and Cr(VI) concentrations in an aqueous solution were effectively reduced in the hybrid field-gradient magnetic separation device. However, a decrease in the saturation adsorption capacity of the magnetic particles was evident for both components in the mixed metal solution relative to the absorption capacities measured when the single metal solutions were evaluated. The differences are attributed to competitive adsorption at active sites. Electrostatic interaction induced selectivity favors selective adsorption of Cr(VI) from the mixture. Adsorption data fit well to the Langmuir isotherm except for As(V) in a mixture. Metal removal of 58.3% for Cr(VI), 37.6% for As(V), and 53% for Cr(VI), and 33.3% for As(V) in a mixture was obtained in one pass of the reactor with stage efficiencies greater than 50%. At 25 ml/min flow rate there is an optimum loading of magnetic particles that maximizes the removal of target ions. Stage efficiency could be improved by having a longer chamber to achieve sufficient residence time at the maximum sustainable flow rate. The MIEX® particles used in this work could be regenerated with an efficiency of more than 75% in all cases. Magnetic particles were characterized to get their hysteresis behavior. The paramagnetic nature of magnetic particles facilitates their regeneration. The saturation magnetization of MIEX particles was found to be 17 EMU/g.

ACKNOWLEDGEMENTS

Financial support for this work was provided by the Department of Energy (grant DE-FG02-04ER86186). We thank A.C. Nunes for useful discussions.

REFERENCES

1. Safarik, I., Safarikova, M., and Forsythe, S.J. (1995) The application of magnetic separations in applied microbiology. *J. Appl. Bacteriol.*, 78 (6): 575–585.
2. Rosensweig, R.E. (1985) *Ferrohydrodynamics*; Cambridge University Press: New York.
3. Zborowski, M., Sun, L., Moore, L.R., Williams, P.S., and Chalmers, J.J. (1999) Continuous cell separation using novel magnetic quadrupole flow sorter. *J. Magn. Magn. Mater.*, 194 (1–3): 224–230.
4. Chalmers, J.J., Zborowski, M., Sun, L., and Moore, L.R. (1998) Flow through, immunomagnetic cell separation. *Biotechnol. Prog.*, 14 (1): 141–148.
5. Ghebremeskel, A.N. and Bose, A.A. (2000) Flow-through, hybrid magnetic-field-gradient, rotating wall device for magnetic colloidal separations. *Sep. Sci. Technol.*, 35 (12): 1811–1826.
6. Ghebremeskel, A.N. and Bose, A. (2002) Magnetic colloid mediated recovery of cadmium ions from an aqueous solution using a flow-through hybrid field-gradient device. *Sep. Sci. Technol.*, 37 (3): 555–569.
7. Ghebremeskel, A.N. and Bose, A. (2003) A continuous, hybrid field-gradient device for magnetic colloid-based separations. *J. Magn. Magn. Mater.*, 261 (1–2): 66–72.
8. Al-Enezi, G., Hamoda, M.F., and Fawzi, N. (2004) Ion exchange extraction of heavy metals from wastewater sludges. *J. Environ. Sci. and Health*, A39 (2): 455.
9. National Research Council. (1999) *Arsenic in Drinking Water*; National Academy Press: Washington, DC, 305.
10. U.S. Environmental Protection Agency. (1998) Toxicological Review of Hexavalent Chromium. National Center for Environmental Assessment, Office of Research and Development. Washington, DC.
11. Tarasevich, Y.I. (2001) Porous structure and adsorption properties of natural porous coal. Colloids and surfaces. A. *Physicochemical and Engineering Aspects*, 176 (2): 267–272.
12. Raji, C. and Anirudhan, T.S. (1997) Chromium (VI) adsorption by sawdust: Kinetics and equilibrium. *Indian Journal of Chemical Technology*, 4 (5): 228–236.
13. Pierce, M.L. and Moore, C.B. (1980) Adsorption of arsenite on amorphous iron hydroxide from dilute aqueous solution. *Environ. Sci. Technol.*, 14 (2): 214–216.
14. Bhattacharyya, D., Jumawan, A.B., and Grieves, R.B. (1979) Separation of toxic heavy metals by sulfide precipitation. *Sep. Sci. Technol.*, 14: 441–452.
15. Pourbaix, M. (1966) *Atlas of Electrochemical Equilibria in Aqueous Solutions;* Pergamon Press: Oxford.
16. Seki, H., Suzuki, A., and Maruyama, H. (2005) Biosorption of chromium(VI) and arsenic(V) onto methylated yeast biomass. *Journal of Colloid and Interface Science*, 281 (2): 261–266.
17. Srivastava, P., Singh, B., and Angove, M. (2005) Competitive adsorption behavior of heavy metals on kaolinite. *Journal of Colloid and Interface Science*, 290 (1): 28–38.
18. Israelachvili, J.N. (1985) *Intermolecular and Surface Forces*; Academic Press: San Diego.

19. Singh, D.B., Prasad, G., and Rupainwar, D.C. (1996) Adsorption technique for the treatment of As(V)-rich effluents. *Colloids and Surfaces A: Physicochemical and Engineering Aspects*, 111 (1–2): 49–56.
20. Karthikeyan, T., Rajgopal, S., and Miranda, LR. (2005) Chromium(VI) adsorption from aqueous solution by *Hevea brasilinesis* sawdust activated carbon. *Journal of Hazardous Materials*, 124 (1–3): 192–199.
21. Khezami, L. and Capart, R. (2005) Removal of chromium(VI) from aqueous solution by activated carbons: Kinetic and equilibrium studies. *Journal of Hazardous Materials*, 123 (1–3): 223–231.